OPEN

Potential Applications of Using ^{68}Ga–Evans Blue PET/CT in the Evaluation of Lymphatic Disorder

Preliminary Observations

Wei Zhang, MD, Peilin Wu, MD,* Fang Li, MD,* Guansheng Tong, MD,† Xiaoyuan Chen, PhD,‡ and Zhaohui Zhu, MD, PhD**

Purpose: Potentials of ^{68}Ga-NEB as a PET tracer in the evaluation of a variety of lymphatic drainage disorders were analyzed.

Methods: ^{68}Ga-NEB was injected subcutaneously, and the PET/CT images were acquired in 13 patients with different suspected lymphatic drainage abnormality. The ^{68}Ga-NEB PET/CT findings were compared with ^{99m}Tc-SC lymphoscintigraphy.

Results: ^{68}Ga-NEB activity could be clearly observed in the lymphatic route on the PET/CT images from all the patients. In 5 (38.5%) of 13 patients tested, ^{68}Ga-NEB PET/CT provided more information than the ^{99m}Tc-SC lymphoscintigraphy.

Conclusions: ^{68}Ga-NEB PET/CT can be used as an alternative of ^{99m}Tc-SC lymphoscintigraphy in the evaluation of lymphatic disorders, which enables fast results and might be more accurate than the conventional ^{99m}Tc-SC lymphoscintigraphy.

Key Words: ^{68}Ga, chyloperitoneum, chylothorax, Evans blue, lymphangioleiomyomatosis, lymphedema, chylothorax, chyloperitoneum, lymphoscintigraphy, PET/CT

(*Clin Nucl Med* 2016;41: 302–308)

Disorders of the lymphatic system are diverse and include lymphedema, chyloperitoneum, chyluria, and chylothorax. Lymphoscintigraphy using ^{99m}Tc-SC is inexpensive with a safety profile and has long been used in the evaluation of pathologies involving lymphatic drainage.[1–7] However, ^{99m}Tc-SC scintigraphy also has several disadvantages, including minimal absorption from the injection site and slow transport from the injection site after subcutaneous administration.[8] Evans blue dye is used for the determination of plasma volume and map for the drainage basins of sentinel node localization.[9] It has fast rate of migration through the lymphatic channels when subcutaneously administered.[9] It is reported before that when scintigraphy and Evans blue dye are used in tandem, false-negative rate for sentinel node localization is decreased compared with using either agent alone.[10]

Received for publication December 29, 2015; revision accepted January 3, 2016.
From the *Department of Nuclear Medicine, Peking Union Medical College Hospital, Chinese Academy of Medical Sciences and Peking Union Medical College; †Department of Nuclear Medicine, Beijing Shijitan Hospital, Capital Medical University, Beijing, People's Republic of China; and ‡Laboratory of Molecular Imaging and Nanomedicine, National Institute of Biomedical Imaging and Bioengineering, National Institutes of Health, Bethesda, MD.
Conflicts of interest and sources of funding: none declared.
Correspondence to: Zhaohui Zhu, MD, PhD, Department of Nuclear Medicine, Peking Union Medical College Hospital, No. 1 Shuaifuyuan, Wangfujing St, Dongcheng District, Beijing 100730, People's Republic of China. E-mail: zhuzhh@pumch.cn; Xiaoyuan Chen, PhD, National Institutes of Health, 35A Convent Dr, GD937, Bethesda, MD 20892. E-mail: shawn.chen@nih.gov.

ISSN: 0363-9762/16/4104–0302
DOI: 10.1097/RLU.0000000000001171

Previous studies have reported the ^{99m}Tc-labeled Evans blue (^{99m}Tc-EB) for lymphatic mapping in animal models.[11–14] It demonstrated that ^{99m}Tc-EB had the same pharmacodynamic properties as Evans blue when incorporated into the cells of the lymph node or became bound to the parenchyma in the lymphatic system. However, those studies also found its limitation in visualizing deep lymph nodes.[13] A recent report showed that ^{18}F-AlF-NEB can distinguish lymph nodes by the apparent blue color and high=intensity PET signal in both inflammation and orthotropic breast cancer animal models.[15] More recently, NOTA-conjugated truncated Evans blue was labeled with ^{68}Ga-NEB and tested for its safety and diagnosis of hepatic hemangioma using PET/CT.[16] In this current investigation, which was approved by the institutional review board of our hospital, we tried to assess the ^{68}Ga-NEB PET/CT in the evaluation of lymphatic disorders.

METHODS AND PATIENTS

Patients and Methods

A total of 13 patients (5 men, 8 women; aged 17–66 years [41 ± 16 years]) were recruited in the analysis. These included 3 patients with lymphedema without known causes. Another 3 patients had postsurgical limb swelling (1 after mastectomy for breast cancer and 2 after oophorectomy for ovary cancers). Seven patients had other types of chyle leak including chylothorax, chyloperitoneum, and chyluria determined by the referring physicians (Table 1). The chylothorax, chyloperitoneum, and chyluria were confirmed by laboratory examination. All of them underwent both ^{68}Ga-NEB PET/CT and ^{99m}Tc-SC scintigraphy within 2 days of each other for suspected lymphatic system disorders. The exclusion criteria included the following: liver and kidney function impairment, low white blood cell count, or currently pregnant or breast-feeding. All patients signed a written informed consent form and were informed of the potential benefits and risks of participating in the investigation.

^{99m}Tc-SC Scintigraphy

Within 2 days of ^{68}Ga-NEB PET/CT, ^{99m}Tc-SC lymphoscintigraphy was performed. For most patients, the tracer was injected into first and second interdigital spaces of both feet (0.5 mL, 37 MBq). For the patient with upper limb swelling (patient 1), the tracer was administered subcutaneously between the thumb and index finger of each hand. Images were acquired with a double-head gamma camera with a low-energy high-resolution parallel whole collimator in whole-body scanning mode at a speed of 10 cm/min. Spot and whole-body images are obtained for up to 24 hours if necessary. The images were read jointly by 2 experienced nuclear medicine physicians.

^{68}Ga-NEB PET/CT

All patients underwent ^{68}Ga-NEB PET/CT. Preparation of NEB and ^{68}Ga labeling were performed as described in previous publications.[17] A Biograph 64 True Point TrueV PET/CT system

TABLE 1. Patient Characteristics

Patient No.	Age, y	Sex	Prescan Indications
1	44	Female	Postmastectomy chest wall swelling
2	34	Male	Chyluria
3	43	Male	Pleural effusion
4	17	Male	Ascites
5	42	Female	Right thigh swelling after ovarian cancer resection
6	43	Female	Leg swelling of unknown causes
7	61	Female	Left leg swelling after ovarian cancer resection.
8	58	Female	Pleural effusion
9	66	Female	Chyluria
10	21	Male	Pleural effusion
11	25	Female	Pleural effusion
12	54	Male	Left leg swelling
13	20	Female	Chyluria

(Siemens Medical Solutions, Erlangen, Germany) was used. For the patient with upper extremity swelling, the tracer (0.5 mL, 37 MBq/hand) was injected into the subcutaneous tissue between the thumb and index finger of each hand. For other patients, ^{68}Ga-NEB was injected subcutaneously into the bilateral first web spaces of the feet (0.5 mL, 37 MBq/foot), followed by massage of the injection sites. The patients were requested to walk after tracer injection. For those patients with suspected chylothorax, chyloperitoneum, or chyluria, the images were acquired 5 to 20 minutes after tracer injection. For those with lymphedema, longer interval up to 1 hour between the tracer injection and image acquisition was applied. Whole-body images were acquired using a low-dose CT scan (120– kV, 35 mA, 3-mm layer, 512 × 512 matrix, 70 cm FOV). PET acquisition was performed (8–11 bed positions, 2 min/bed).

RESULTS

^{68}Ga-NEB Distribution

^{68}Ga-NEB activity can clearly visualize lymphatic vessels and lymph nodes by PET/CT in all patients. Distribution of ^{68}Ga NEB was also found in the heart and major vessels. Renal and hepatic activity gradually increased radioactivity over time. The spleen can also have mild activity.

Time Differences Between ^{99m}Tc-SC Lymphoscintigraphy and ^{68}Ga-NEB PET/CT in Acquiring Sufficient Information for Diagnosis

^{68}Ga NEB PET/CT needs significantly less time waiting after tracer injection to perform than the ^{99m}Tc-SC lymphoscintigraphy.

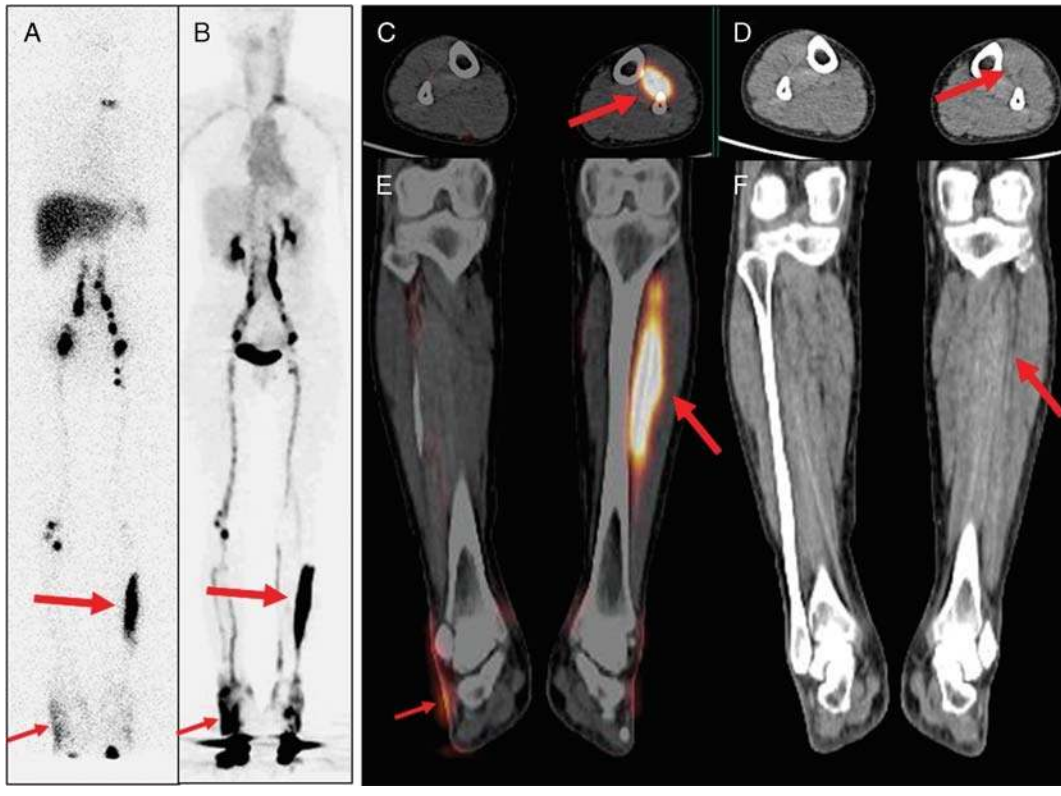

FIGURE 1. A 43-year-old woman (patient 6) with symptoms of swollen lower limbs for more than 4 years. Both anterior ^{99m}Tc-SC scintigraphy (**A**) and ^{68}Ga-NEB PET/CT MIP image (**B**) acquired 60 minutes after tracer injection showed dermal backflow on bilateral ankles and feet (small arrows) and lateral left calf (large arrows). On both transaxial (**C** and **D**) and coronal (**E** and **F**) images of ^{68}Ga-NEB PET/CT, the abnormal radioactivity accumulation corresponded to tubular low density (large arrows), which was consistent with a diagnosis of lymphatic cyst. Dermal backflow in the feet/ankle was also clearly visualized on the tomographic image (**E**: small arrow).

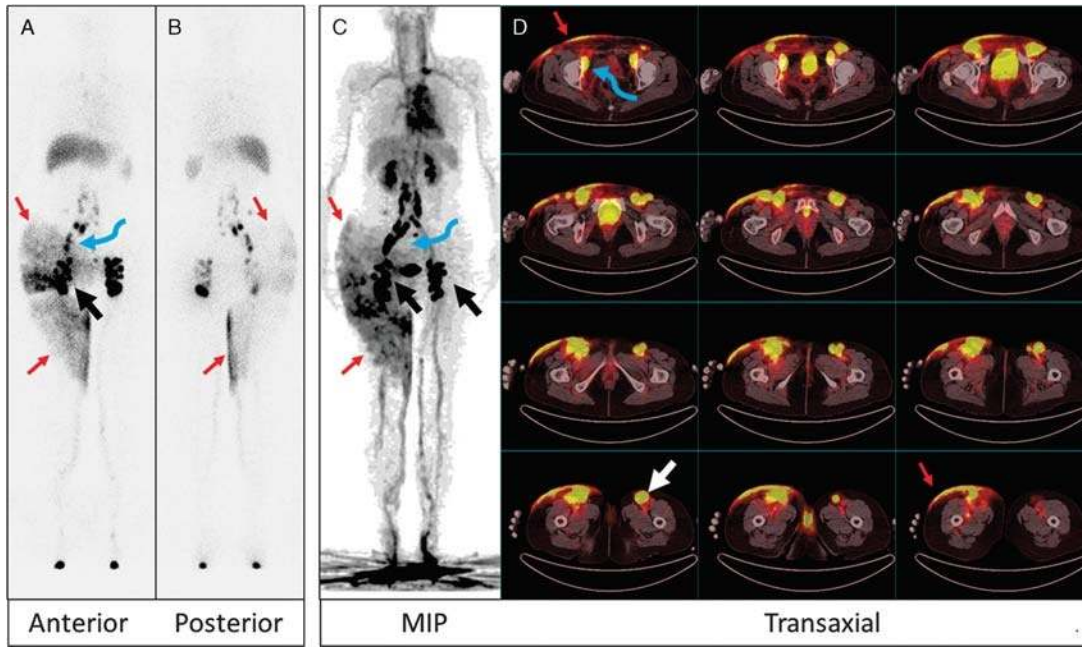

FIGURE 2. A 42-year-old woman (patient 5) developed swelling in her right upper thigh and right lower abdomen and pelvis after total abdominal hysterectomy with bilateral salpingo-oophorectomy due to ovary cancer. On both anterior (**A**) and posterior (**B**) images of ^{99m}Tc-SC scintigraphy acquired 5 hours after injection, there was significant dermal backflow (thin red arrows) in the right lower abdomen/right pelvis and right thigh, consistent with lymphedema and the clinical symptoms. Inguinal nodes (thick arrow) and right iliac nodes (curved arrow) were also noted. Similar findings could be found on the MIP image (**C**) of ^{68}Ga-NEB PET, which was acquired 1 hour after tracer injection. All findings (dermal backflow: thin red arrow; inguinal nodes: thick arrows; and iliac nodes: curved arrow) were better appreciated on transaxial fusion images (**D**) of ^{68}Ga-NEB PET/CT.

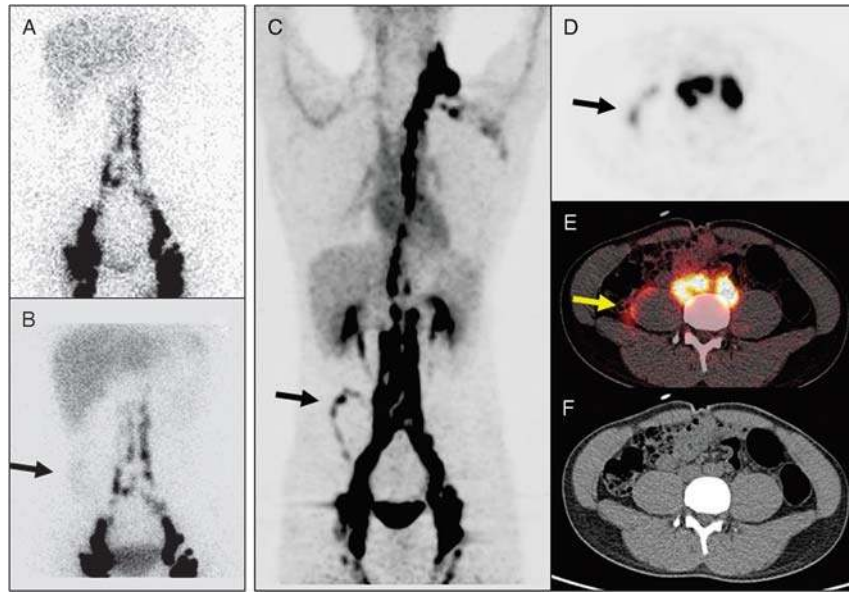

FIGURE 3. A 17-year-old man (patient 4) with abdominal discomfort for more than 6 months. Chylous ascites was suspected, and nuclear medicine was consulted. ^{99m}Tc-SC anterior image of the abdomen acquired 60 minutes after injection (**A**) was unremarkable. The image acquired 6 hours after injection (**B**), however, revealed diffuse, mild radioactivity on the right side of the lower abdomen (arrow). On ^{68}Ga-NEB MIP image (**C**) acquired 5 minutes after tracer injection, clear linear activity (arrow) could be seen in the right abdomen. On transaxial PET (**D**), fusion (**E**), and CT (**F**) images, this activity (arrows) was located in the immediate anterolateral border of the right psoas muscle, indicating the site of the chyle leak. Intense activity in the inguinal, iliac, and paraspinal lymph nodes and thoracic duct was also better appreciated on ^{68}Ga-NEB PET/CT images.

In our patient population, the ^{68}Ga NEB PET/CT images were acquired between 10 and 90 minutes after tracer administration. In comparison, the images of ^{99m}Tc-SC lymphoscintigraphy had to be acquired much later. The time of completing image acquisition after tracer injection is 0.9 ± 0.2 hour (mean ± SD) for ^{68}Ga NEB PET/CT scan, which is significantly shorter ($P < 0.01$) than for the ^{99m}Tc-SC lymphoscintigraphy (7.8 ± 6.9 hours).

Image Findings Between ^{99m}Tc-SC Lymphoscintigraphy and ^{68}Ga NEB PET/CT

Among all 13 patients, the results of ^{99m}Tc-SC lymphoscintigraphy and ^{68}Ga NEB PET/CT were consistent in 8 of them (Figs. 1, 2), although the results of ^{68}Ga NEB PET/CT were obtained much faster. ^{68}Ga NEB PET/CT provided more information in 5 patients (38.5%). In 1 patient with chyloperitoneum, ^{99m}Tc-SC lymphoscintigraphy was unable to localize the site of the chyle leak, whereas ^{68}Ga NEB PET/CT successfully identified leak (Fig. 3). In 2 patients with chylothorax, ^{99m}Tc-SC lymphoscintigraphy was unable to identify the sites of the leak. In contrast, the sites of the leakage were found after ^{68}Ga-NEB PET/CT (Fig. 4). In 1 patient who had postsurgical limp swelling, the site of the chyle leak was identified only by ^{68}Ga-NEB PET/CT but not by ^{99m}Tc-SC lymphoscintigraphy (Fig. 5). In a young female patient who had cystic lesions and pleural effusion, the site of chest abnormality was visualized on ^{68}Ga-NEB PET/CT but not on ^{99m}Tc-SC lymphoscintigraphy (Fig. 6). The abdominal and pelvic lesions of the same patient were also better visualized by ^{68}Ga-NEB study than the ^{99m}Tc-SC images (Figs. 6, 7). A diagnosis of lymphangioleiomyomatosis, a rare slowly progressive, low-grade, metastasizing neoplasm of women that spreads primarily through the lymphatic channels,[18,19] was subsequently made in this patient.

DISCUSSION

Evans blue dye is usually used in defining the drainage basins and mapping for the localization of tumor sentinel node before surgery. When Evans blue diffuses into the cellular matrix, it binds to endogenous proteins forming an Evans blue–protein complex, which can specifically penetrate the single layers of gracile lymphatic endothelial cells, but does not migrate into the venous capillary network as the size of the complex is too large to enter arteriovenous capillaries.[20–23] Our results show that ^{68}Ga-NEB can be clearly observed in the lymphatic vessels and lymph nodes on the PET/CT images of the patients, which shows similar migration properties as Evans blue and ^{99m}Tc-labeled Evans.[11–13] Evans blue is known to be metabolized in the liver by cytochrome C (P450) reductase and then excreted through the renal route as colorless, radioactive metabolites.[24] We also observed slight distribution of radioactivity in the liver and prominent visualization of the kidneys over time on ^{68}Ga-NEB PET/CT scans. The cardiac blood pool and spleen also had radioactivity distribution. In our patient population, when comparing with ^{99m}Tc-SC lymphoscintigraphy, ^{68}Ga NEB PET/CT can be completed much faster. This is because ^{99m}Tc-SC lymphoscintigraphy requires long waiting time before scan can be completed because of the problem that the radiolabeled SCs are relatively large particle sizes that do not move effectively. In addition, ^{68}Ga-NEB PET/CT appears more revealing than ^{99m}Tc-SC lymphoscintigraphy because in 30.7% (4/13) patients ^{68}Ga NEB PET/CT presented more clinically important information than did ^{99m}Tc-SC lymphoscintigraphy. This is conceivable because ^{68}Ga NEB PET/CT images are 3-dimensional and have CT to correlation, whereas traditional ^{99m}Tc-SC lymphoscintigraphy acquires only static images without CT correlation, which has intrinsic disadvantage compared with PET/CT.

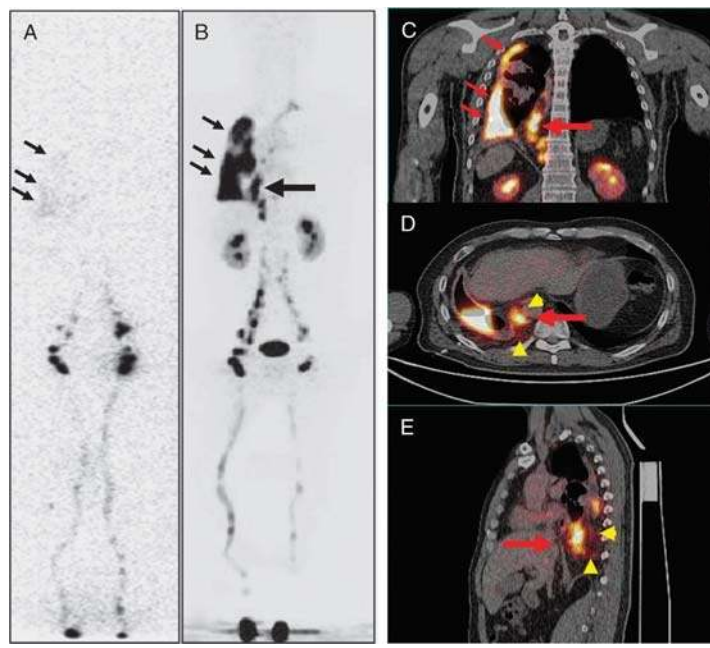

FIGURE 4. A 43-year-old man with the right side of persistent pleural effusion (patient 3). The patient had a remote history of motor vehicle accident. Laboratory examination of the fluid after thoracocentesis demonstrated chylothorax. ^{99m}Tc-SC scintigraphy (**A**) revealed diffuse, mild activity in the right chest, consistent with the clinical findings of right chylothorax. However, the potential site of the chyle leak could not be identified. In comparison, ^{68}Ga-NEB PET/CT (**B**, MIP; **C**: coronal fusion; **D**: axial fusion; **E**: sagittal fusion) not only showed activity in the right chest pleural effusion (small arrows), but also clearly revealed an additional vertically linear intense activity (large arrow) centered in the dilated thoracic duct and cisterna chyli with mild activity surrounding (arrowheads), consistent with the site of the leak.

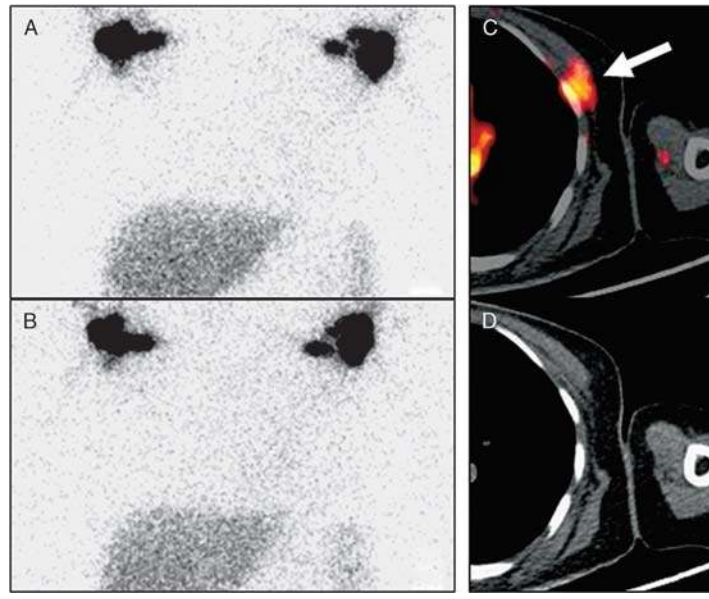

FIGURE 5. Anterior ^{99m}Tc-SC images were acquired at 2 hours (**A**) and 6 hours (**B**) after subcutaneous tracer injection between the thumb and index finger of the hands in a 44-year-old woman (patient 1) who had left chest swelling and was status post left mastectomy for breast cancer. The images revealed axillary lymph nodes bilaterally and minimally more tracer activity in the left chest without evidence of the site of the leak. In comparison, the transaxial images (**C**: fusion; **D**: CT) of the ^{68}Ga-NEB PET/CT acquired at 30 minutes after injection demonstrated a focal activity (arrow) underneath the left pectoralis major muscle, at the level of the left anterior fourth rib, indicating the site of the chyle leak.

We feel that much faster moving of ^{68}Ga-NEB along the lymphatic route itself at least also plays a role in increasing the accuracy of the study. When ^{99m}Tc-SC slowly leaked over several hours, the leaked radioactivity could spread to a larger region, which might obscure the true site of the leak (Figs. 3B, 8A). In contrast, the high concentration of ^{68}Ga-NEB activity at the leak site can be determined prior to the activity diffused into adjacent region (Figs. 3C–E, 8B, C). This difference between speeds of moving

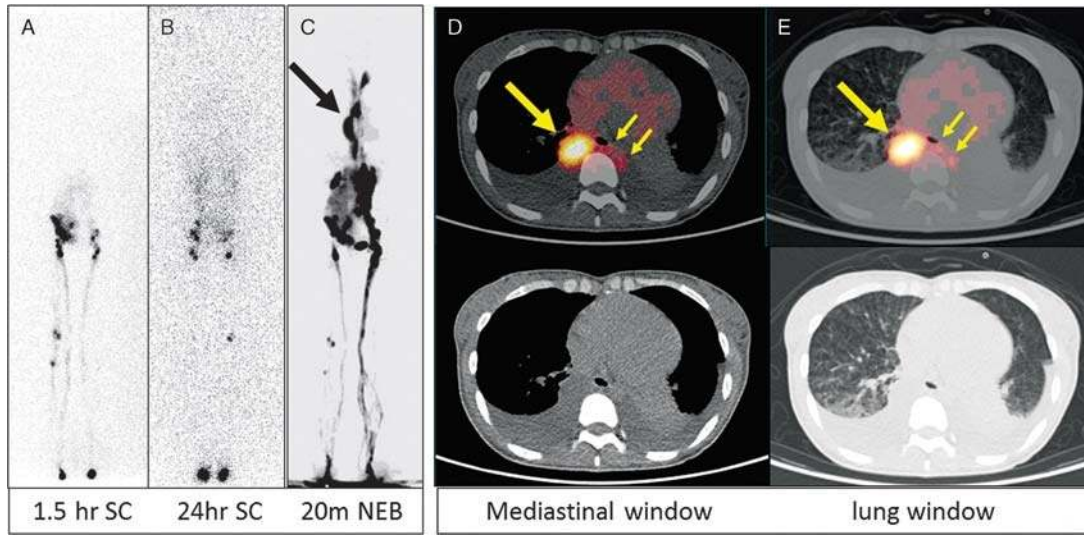

FIGURE 6. A 25-year-old woman presented with shortness of breath for 3 months (patient 11). A diagnostic CT (images not shown) revealed many cystic structures in the chest, abdomen, and pelvis. In addition, bilateral pleural effusion was noted, which was subsequently shown as chylothorax. For this reason, lymphoscintigraphy was ordered. The ^{99m}Tc-SC images at 1.5 hours (**A**) and 24 hours (**B**) after injection in the feet both showed that the tracer reached abdomen/pelvis without much chest activity. However, on ^{68}Ga-NEB MIP PET image (**C**) acquired 20 minutes after tracer injection, there was clear, intense vertical activity (large arrow) in the thorax. On transaxial images (**D**: mediastinal window; **E**: lung window), the vertical activity was in an enlarged thoracic duct (large arrows). The chyle leak (small arrows) from the thoracic duct to the left chest was also noted. There were also many small cysts in both lungs (**E**).

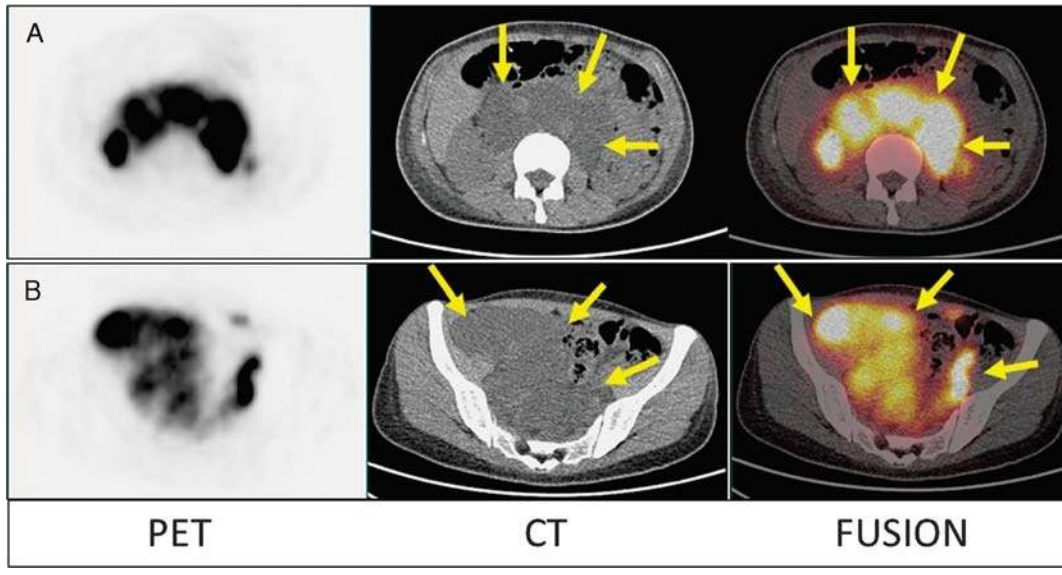

FIGURE 7. Furthermore, the transaxial images of the abdomen (**A**) and pelvis (**B**) of ^{68}Ga-NEB PET/CT from the same patient demonstrated that all of the hypodense cystic structures were filled with radioactive lymph fluid (small arrows), which was not impressively seen on ^{99m}Tc-SC scintigraphy. Eventually, the patient was proven to have lymphangioleiomyomatosis.

along the lymphatic route between these 2 tracers might also be a contributor of higher accuracy of ^{68}Ga-NEB PET/CT.

Many publications in recent years have shown that adding SPECT/CT images to routine planar ^{99m}Tc-SC lymphoscintigraphy can significantly add diagnostic value of the study.[25–30] However, ^{68}Ga NEB PET/CT still has advantage over ^{99m}Tc-SC lymphoscintigraphy with SPECT/CT image acquisition. For example, acquisition of images covering from feet to the shoulder is generally necessary to evaluate different lymphatic drainage disorders. However, it takes only approximately 20 minutes for modern PET/CT scanner to acquire images from feet to the neck. In contrast, it needs several hours to acquire multiple bed position SPECT/CT images. Long time under scanner is causing not only inconvenience to the patients and nuclear medicine technologists, but also a source of mismatch between SPECT and CT images because patient movement becomes difficult to avoid during very long scanning time. In addition, SPECT/CT images per se will be unable to solve the necessary long-waiting period between the ^{99m}Tc-SC injection and final image acquisition.

CONCLUSION

^{68}Ga-NEB PET/CT is a promising technique in the evaluation of lymphatic drainage abnormality, which can reach the

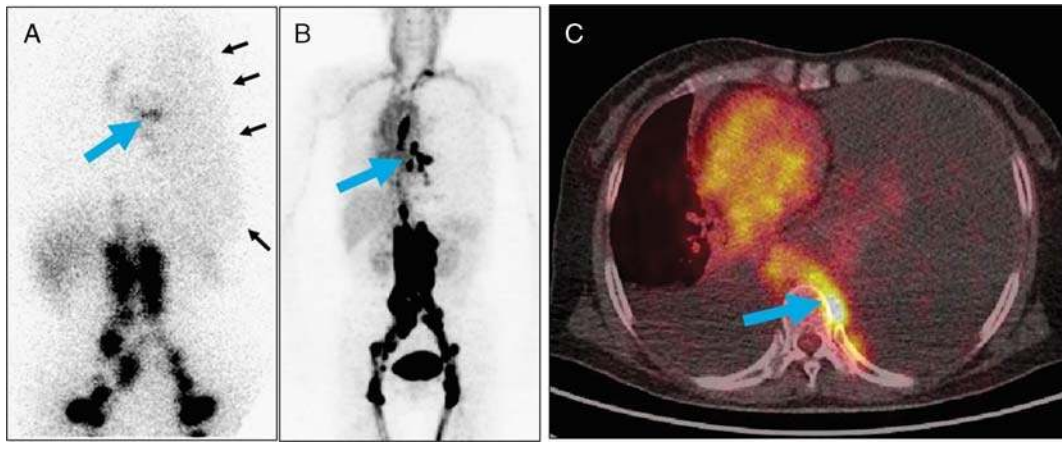

FIGURE 8. A 58-year-old woman (patient 8) presented with chest tightness for 8 months. Routine examination revealed pleural effusion in both sides of the thorax, more severe on the left side. Laboratory examination of thoracocentesis drainage confirmed chylothorax. ^{99m}Tc-SC scintigraphy (**A**) at 1 hour after injection showed relatively focal radioactivity (large arrow) in the left middle chest. In addition, mild, diffuse radioactivity (small arrows) in the entire left thorax was noted. The abnormal radioactivity distribution in the left mediastinal area is much more obvious on ^{68}Ga-MIP image (**B**) of NEB PET/CT acquired 15 minutes after tracer injection. Interestingly, the activity in the left pleural effusion was not as obvious on PET images as the ^{99m}Tc-SC image (compared with **A**). The PET/CT fusion image demonstrated that this activity (large arrow) was on the left of T7 vertebral body (**C**).

diagnosis much earlier than the conventional ^{99m}Tc-SC lymphoscintigraphy and is also possibly more accurate. However, more comparison studies that include SPECT/CT images in ^{99m}Tc-SC lymphoscintigraphy are necessary to determine whether ^{68}Ga-NEB PET/CT is more accurate than ^{99m}Tc-SC lymphoscintigraphy with SPECT/CT.

REFERENCES

1. Witte MH, Williams WH. Chylothorax and chyloperitoneum. *N Engl J Med*. 2006;354:879; author reply 879.
2. Kazemzadeh GH, Sadeghi R, Ebrahimi E, et al. A successful experience in managing a chylous reflux: importance of lymphoscintigraphy. *Clin Nucl Med*. 2014;39:485–487.
3. Kim DW, Kim MH, Kim CG. Lymphoscintigraphy revealed chyloperitoneum after gastrectomy for gastric cancer. *Clin Nucl Med*. 2015;40:41–44.
4. Pui MH, Yueh TC. Lymphoscintigraphy in chyluria, chyloperitoneum and chylothorax. *J Nucl Med*. 1998;39:1292–1296.
5. Pena Quian Y, Hernandez Ramirez P, Batista Cuellar JF, et al. Lymphoscintigraphy for the assessment of autologous stem cell implantation in chronic lymphedema. *Clin Nucl Med*. 2015;40:217–219.
6. Bender B, Murthy V, Chamberlain RS. The changing management of chylothorax in the modern era. *Eur J Cardiothorac Surg*. 2016;49:18–24.
7. Oh JK, Yoon HE, Chung YA. Lymphoscintigraphic demonstration of chyle leak after kidney transplantation and gamma camera detection of radioactivity in chylous aspirate. *Clin Nucl Med*. 2014;39:760–761.
8. Hung JC, Wiseman GA, Wahner HW, et al. Filtered technetium-99m-sulfur colloid evaluated for lymphoscintigraphy. *J Nucl Med*. 1995;36:1895–1901.
9. Margouleff D. Blood volume determination, a nuclear medicine test in evolution. *Clin Nucl Med*. 2013;38:534–537.
10. Wong SL, Edwards MJ, Chao C, et al. Sentinel lymph node biopsy for breast cancer: impact of the number of sentinel nodes removed on the false-negative rate. *J Am Coll Surg*. 2001;192:684–689; discussion 689–691.
11. Green M, Farshid G, Kollias J, et al. The tissue distribution of Evans blue dye in a sheep model of sentinel node biopsy. *Nucl Med Commun*. 2006; 27:695–700.
12. Sutton R, Tsopelas C, Kollias J, et al. Sentinel node biopsy and lymphoscintigraphy with a technetium 99m labeled blue dye in a rabbit model. *Surgery*. 2002;131:44–49.
13. Tsopelas C, Bellon M, Bevington E, et al. Lymphatic mapping with ^{99m}Tc-Evans blue dye in sheep. *Ann Nucl Med*. 2008;22:777–785.
14. Tsopelas C, Bevington E, Kollias J, et al. ^{99m}Tc-Evans blue dye for mapping contiguous lymph node sequences and discriminating the sentinel lymph node in an ovine model. *Ann Surg Oncol*. 2006;13:692–700.
15. Wang Y, Lang L, Huang P, et al. In vivo albumin labeling and lymphatic imaging. *Proc Natl Acad Sci U S A*. 2015;112:208–213.
16. Zhang J, Lang L, Zhu Z, et al. Clinical translation of an albumin-binding PET radiotracer ^{68}Ga-NEB. *J Nucl Med*. 2015;56:1609–1614.
17. Niu G, Lang L, Kiesewetter DO, et al. In vivo labeling of serum albumin for PET. *J Nucl Med*. 2014;55:1150–1156.
18. Gupta R, Kitaichi M, Inoue Y, et al. Lymphatic manifestations of lymphangioleiomyomatosis. *Lymphology*. 2014;47:106–117.
19. Steagall WK, Taveira-DaSilva AM, Moss J. Clinical and molecular insights into lymphangioleiomyomatosis. *Sarcoidosis Vasc Diffuse Lung Dis*. 2005; 22(suppl 1):S49–S66.
20. Moghimi SM, Bonnemain B. Subcutaneous and intravenous delivery of diagnostic agents to the lymphatic system: applications in lymphoscintigraphy and indirect lymphography. *Adv Drug Deliv Rev*. 1999;37:295–312.
21. Pfister G, Saesseli B, Hoffmann U, et al. Diameters of lymphatic capillaries in patients with different forms of primary lymphedema. *Lymphology*. 1990; 23:140–144.
22. Warren AG, Brorson H, Borud LJ, et al. Lymphedema: a comprehensive review. *Ann Plast Surg*. 2007;59:464–472.
23. Tsopelas C, Sutton R. Why certain dyes are useful for localizing the sentinel lymph node. *J Nucl Med*. 2002;43:1377–1382.
24. Muskhelishvili L, Thompson PA, Kusewitt DF, et al. In situ hybridization and immunohistochemical analysis of cytochrome P450 1B1 expression in human normal tissues. *J Histochem Cytochem*. 2001;49:229–236.
25. Atkinson C, Banks K. Imaging idiopathic chylopericardium with ^{99m}Tc-SC lymphoscintigraphy and SPECT/CT. *Clin Nucl Med*. 2015;40:e508–e510.
26. Baulieu F, Bourgeois P, Maruani A, et al. Contributions of SPECT/CT imaging to the lymphoscintigraphic investigations of the lower limb lymphedema. *Lymphology*. 2013;46:106–119.
27. Han DY, Cheng MF, Yen RF, et al. Postoperative lymphocele demonstrated by lymphoscintigraphy SPECT/CT. *Clin Nucl Med*. 2012;37:374–376.
28. Yang J, Codreanu I, Zhuang H. Minimal lymphatic leakage in an infant with chylothorax detected by lymphoscintigraphy SPECT/CT. *Pediatrics*. 2014;134:e606–e610.
29. Prevot N, Tiffet O, Avet J Jr, et al. Lymphoscintigraphy and SPECT/CT using ^{99m}Tc filtered sulphur colloid in chylothorax. *Eur J Nucl Med Mol Imaging*. 2011;38:1746.
30. Weiss M, Schwarz F, Wallmichrath J, et al. Chylothorax and chylous ascites. Clinical utility of planar scintigraphy and tomographic imaging with SPECT/CT. *Nuklearmedizin*. 2015;54:231–240.